EFFECTIVENESS OF BRISTLED WING OF THRIPS

Ken Sato, Hidetoshi Takahashi, Minh-Dung Nguyen, Kiyoshi Matsumoto, and Isao Shimoyama
The University of Tokyo, Tokyo, JAPAN

ABSTRACT

We have investigated the mechanism of a bristled wing of thrips by using an artificial cantilever-based wing. Five kinds of the artificial bristled wing, which had the similar size of the thrips wing, with a different hair gap were evaluated in a wind tunnel. Experiment results suggested that at low hair-gap-based Reynolds number (<10), the bristled areas of the wing acted as an imaginary airflow block, which increased the aerodynamic force. Meanwhile, this phenomenon did not occur at high Reynolds number (>100).

INTRODUCTION

Recently, the flight mechanism of small insects has attracted much attention. In previous researches, capturing a flapping motion of small insects with a high speed camera have been the major method to clarify their flight mechanism [1,2]. To measure the aerodynamic force or visualize air flow, experiments with dynamically scaled models of the insect wing have been also reported [3,4]. The researches on the flying insects are likely to target the large-scale flying insects like butterfly or dragonfly, whose wing lengths are 5-10 cm. Hence, the flight mechanisms of the small insects whose length is approximately 1 mm are not fully understood.

Among small flying insects, thrips, with body length less than 1 mm, has the characteristic bristled wings which own no membranes between the wing hairs. The illustrations of thrips and bristled wing are shown in Figure 1. The reason why thrips own bristled wings instead of ordinary membrane wings is biologically interesting. Yet the effectiveness of the bristled wings still remains unclear [5-7].

To clarify the flight mechanisms of thrips, several researches have focused on aerodynamic force acting on the bristled wing of thrips. Position, velocity, and movement of bristled wings of thrips during free flight were captured with two set of high speed camera [6]. This experiment was able to indirectly estimate the direction and the magnitude of the aerodynamic force of thrips. To measure this aerodynamic force acting on the bristled wing, Sunada fabricated a dynamical scaled mechanical model of a bristled wing of thrips and measured the fluid-dynamic force [7]. However, the artificial models were limited to be approximately 100 times larger than an actual wing. Additionally, the effectiveness of the bristled wing of thrips was not confirmed quantitatively.

In this paper, to clarify the aerodynamics of the bristled wings in thrips, we proposed an artificial bristled wing based on a piezo-resistive cantilever, which was approximately the same size with the actual wing of thrips (= 1 mm length). The air flow through the hairs of the bristled wing was first numerically analyzed using Finite Element Method (FEM) method. Moreover, we fabricated five kinds of the artificial bristled cantilever with different hair gaps and measured the fractional resistance change of the cantilevers with different airflow velocities.

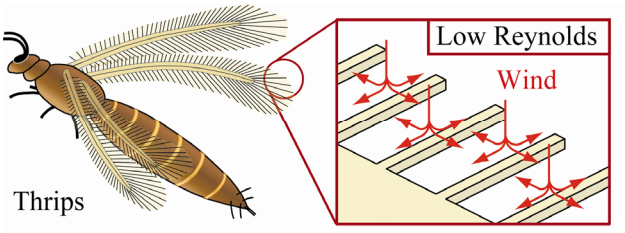

Figure 1: Schematic illustration. No air flow between hairs of the bristled wing of thrips.

We found that for the hair-gap-based Reynolds number less than 10, the bristled areas of the wing acted as an imaginary airflow block. Meanwhile, when the Reynolds number is greater than 100, this phenomenon did not occur.

SENSOR DESIGN AND FABRICATION

The design of the artificial bristled wing is shown in Figure 2(a). This bristled wing was a piezo-resistive cantilever which deformed and changed its resistance when air flow was applied on its surface. The resistance change of the cantilever was proportional to the deformation of the cantilever. This kind of cantilever was studied in previous works of our group, and detail of the mechanism as an airflow sensor was given in [8, 9]

We design the size of the cantilever to be similar to that of thrips wing (Figure 2(a)). Length of the cantilever part with hairs was 1000 μm. Thickness of the cantilevers was 3 μm. In this study, we used five kinds of the cantilevers: one was the rectangle-shaped cantilever (cantilever A) and the others were the bristled cantilevers (cantilever B). Photographs of the fabricated cantilevers were shown in Figure 2(b). In order to know the effect of hair gap on the thrips flight mechanism, we designed the cantilevers B with four different hair gap lengths (60 μm, 130 μm, 300 μm, 900 μm (B1-B4)). The number of hairs in both sides of cantilever B1, B2, B3 and B4 were 16, 8, 4 and 2, respectively. Each cantilever B1, B2, B3 or B4 was compared with cantilever A, which was fabricated on the same chip (Figure 2(c)). For all cantilever B, the ratio between the hair gap and hair width was 8:1 so that their surface areas were the same. The total areas of the cantilevers were 0.32 mm^2 (for cantilever A) and 0.41 mm^2 (for all cantilevers B).

The sensor fabrication process is shown in Figure 3. We used a 3 μm / 2 μm /300 μm thick SOI (silicon on insulator) wafer. First, N-type piezo-resistor was formed on the SOI wafer by rapid thermal diffusion (Figure 3(1)). Second, chrome and gold layers were deposited, and patterned. Using these layers as mask, the topside silicon layer was etched by DRIE (Figure 3(2)). Then the chrome and gold layer was etched again to form the electrodes (Figure 3(3)). The bottom-side silicon layer was etched by

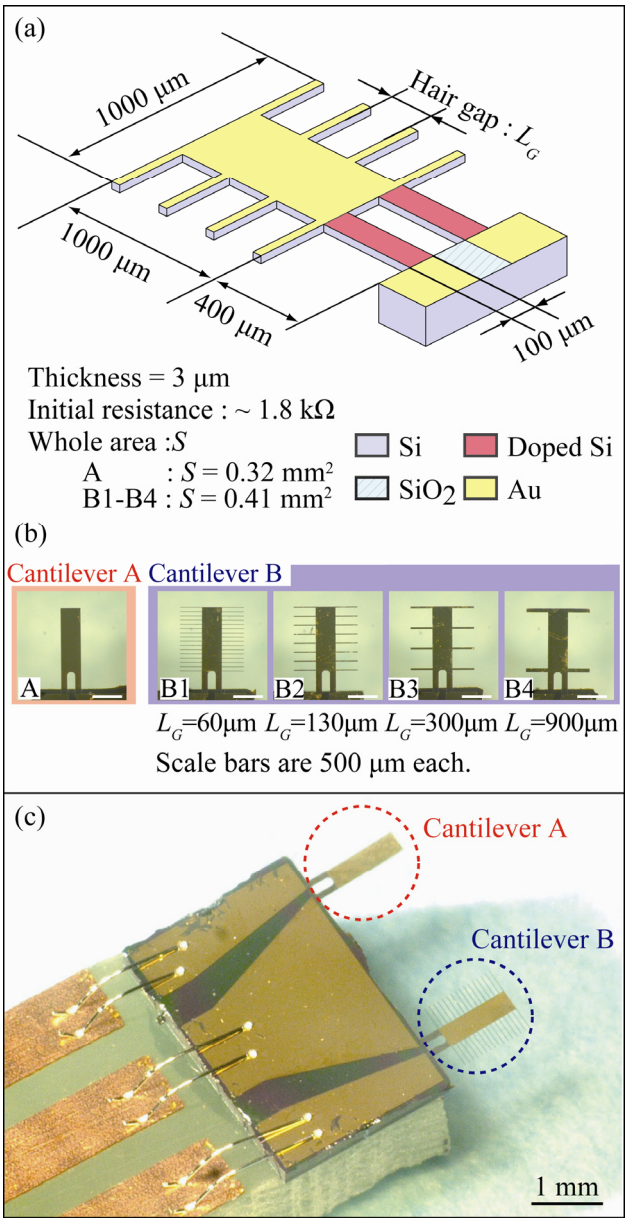

Figure 2: (a) Cantilever design. (b) Photographs of the cantilevers. Scale bars are 500μm each. We used five kinds of cantilevers in this experiment. (c)Photograph of the sensor chip. Cantilever A and cantilever B was placed on one chip.

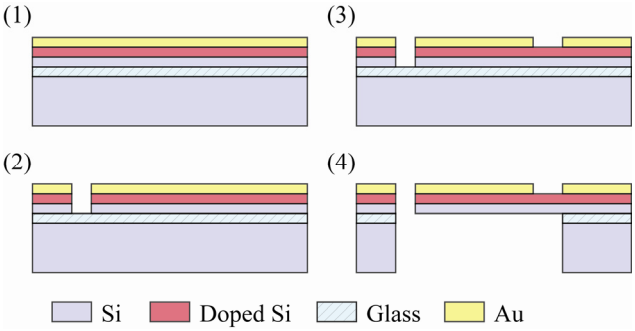

Figure 3: Fabrication process of the sensor. All the cantilevers are fabricated on a same SOI wafer.

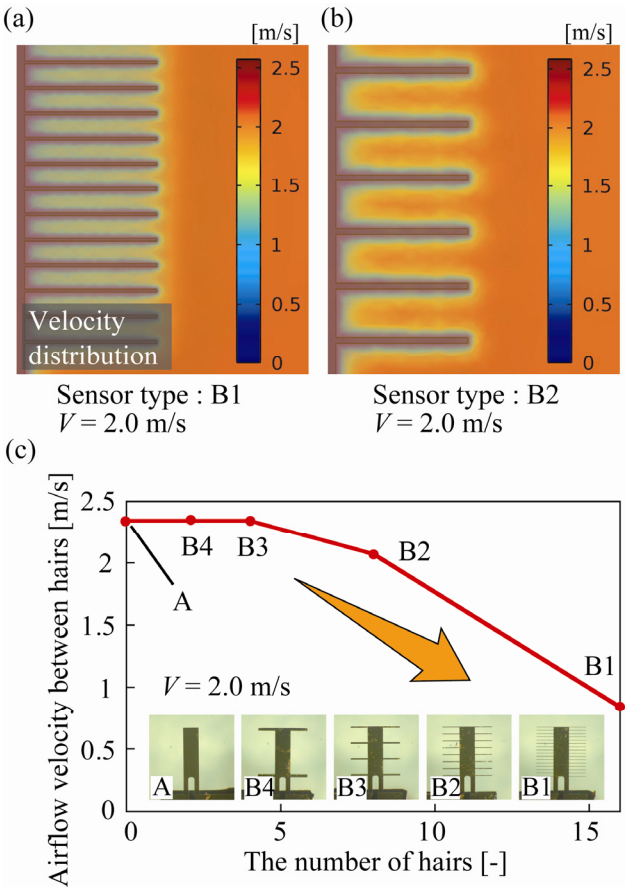

Figure 4: (a),(b) Velocity distribution around the cantilevers when applying air flow of 2.0 m/s. (c) Relationship between number of the hairs and airflow velocity between hairs when applying airflow of 2.0 m/s to the sensor surface.

DRIE from the backside, and the cantilever was released by etching the glass layer in HF vapor (Figure 3(4)). The initial resistances of the cantilevers were about 1.8 kΩ.

SIMULATION RESULT

We carried out the fluid-structure interaction simulation using FEM method (COMSOL Multiphysics).

Figure 4 shows the simulation result of the airflow velocity distribution around the cantilever when applying airflow of 2.0 m/s vertically to the sensor surface. Figure 4(a), (b) shows airflow velocity distribution around cantilever B1 and B2, respectively. These simulation results show that the airflow velocity around the cantilever, especially between the narrower hair gaps, is lower than other places.

Figure 4(c) shows the relationship between the number of hairs and airflow velocity between hairs. Here, the airflow velocity was defined as the velocity of the center point of the hair gap. Notice that all cantilever B1, B2, B3 and B4 in our simulation had the same surface area; only the number of hairs was different. In case of cantilever B3 and B4, the air velocities between the hairs were approximately the same with that of cantilever A. However, as the number of hairs increased, (i.e. the hair gap length decreased), the airflow velocity between the hairs decreased. For example, in the case of cantilever B1,

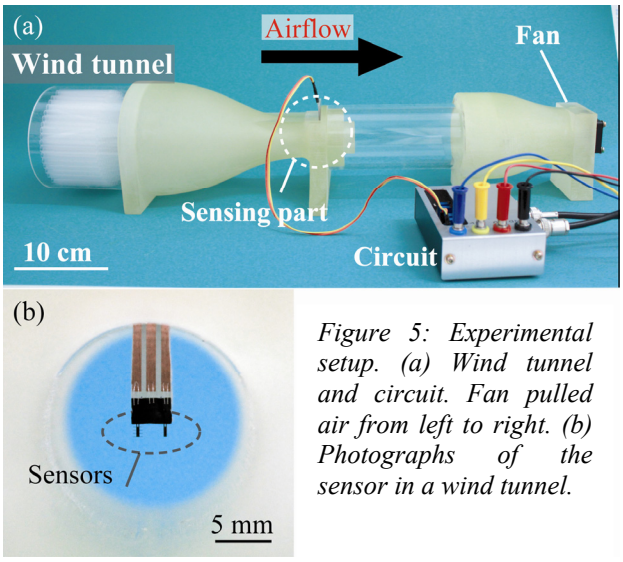

Figure 5: Experimental setup. (a) Wind tunnel and circuit. Fan pulled air from left to right. (b) Photographs of the sensor in a wind tunnel.

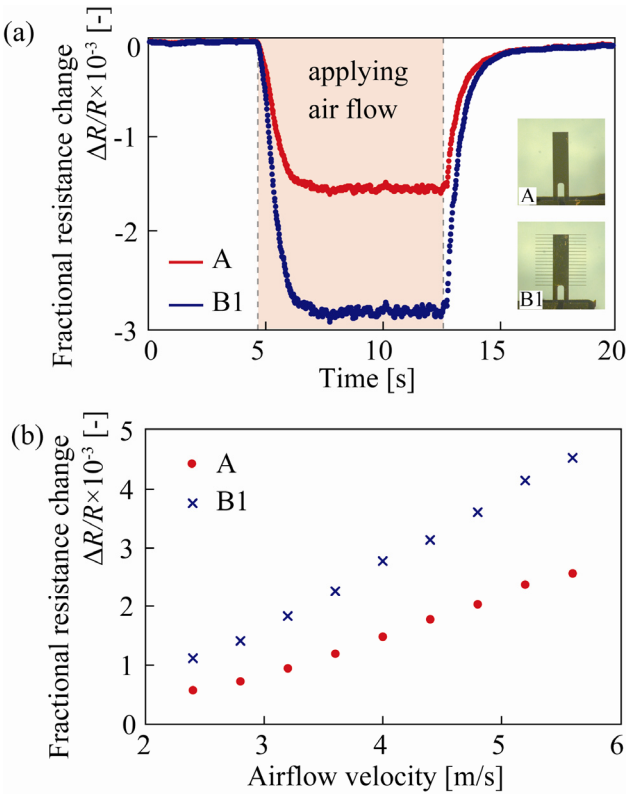

Figure 6: (a) Response of the sensor A and sensor B against air flow of 4.0 m/s. (b) Relationship between airflow velocity and the fractional resistance change of cantilever A and B1.

airflow velocity decreased to 0.84 m/s, which was 36 % of the airflow velocity in case of cantilever A. The simulation results suggest that airflow velocities through the hair gaps decrease as the hair gaps become smaller. This result implies that the narrow gaps of the thrips wing act as imaginary airflow blocks, which increase the drag force on the wing.

EXPERIMENTS AND RESULTS

Figure 5(a) shows the experimental setup to investigate the effect of the hair-gap length on the deformation of the cantilever. The sensor was placed in the middle of a wind tunnel (Figure 5(b)). The airflow velocity could be controled from 2.0 m/s to 6.0 m/s by adjusting the power of the fan.

Figure 6(a) shows the real time response of cantilever A and cantilever B1 to 4.0 m/s airflow. The relationship between airflow velocity and the fractional resistance change of cantilever A and B1 is shown in Figure 6(b). The result shows that even the surface area of cantilever B was only about 1.25 times larger than that of cantilever A, aerodynamic force of cantilever B1 was able to achieve approximately twice larger deformation compared to that of cantilever A ranging airflow velocity of 2.0-6.0 m/s.

Figure 7(a) shows the relationship between the number of hairs and drag coefficient of cantilever A and cantilever B (=C_{DB}/C_{DA}) when applying air flow of 2.0 m/s, 4.0 m/s, and 5.6 m/s. C_{DB}/C_{DA} means the ratio of drag force per area of cantilever A and B. The fractional resistance change was proportional to the drag force since the response of the cantilever is shifted linearly according to drag force. This equation is given by

$$\frac{\Delta R}{R} \propto Drag \tag{1}$$

Drag coefficient (C_D) is given by

$$C_D = \frac{Drag}{(1/2)\rho V^2 S} \tag{2}$$

where ρ is dynamic coefficient of viscosity, S is surface area of the cantilever. From (1), (2) equations, C_{DB}/C_{DA} is derived by

$$\frac{C_{DB}}{C_{DA}} = \frac{\Delta R_B / R_B}{\Delta R_A / R_A} \cdot \frac{S_A}{S_B} \tag{3}$$

According to Figure 7(a), there was positive correlation between the number of hairs and C_{DB}/C_{DA}, which indicated that small hair gaps increased the generated power.

Figure 7(b) shows the relationship between airflow velocity and C_{DB}/C_{DA}. This figure shows two conclusions. The first one is that the bristled wing generated larger drag forces than membrane-shaped wing per unit area. The other is that when the airflow velocity was higher, the effectiveness of drag became lower. Figure 8 shows the relationship between hair-gap-based Reynolds number and C_{DB}/C_{DA}. In this study, hair gap length of the cantilever was defined as an effective length. C_{DB}/C_{DA} was shifted linearly to logarithm of hair-gap-based Reynolds number. At Re =5-10, C_{DB} was 1.5 times larger than C_{DA}. Meanwhile, at Re >100, C_{DB} was 1.1 times larger than C_{DA}. These results suggest that when thrips flying, air does not flow between the hairs and hairs act as a membrane wing. In this way, this study confirms that bristled wing acts as an imaginary airflow block at low Reynolds number.

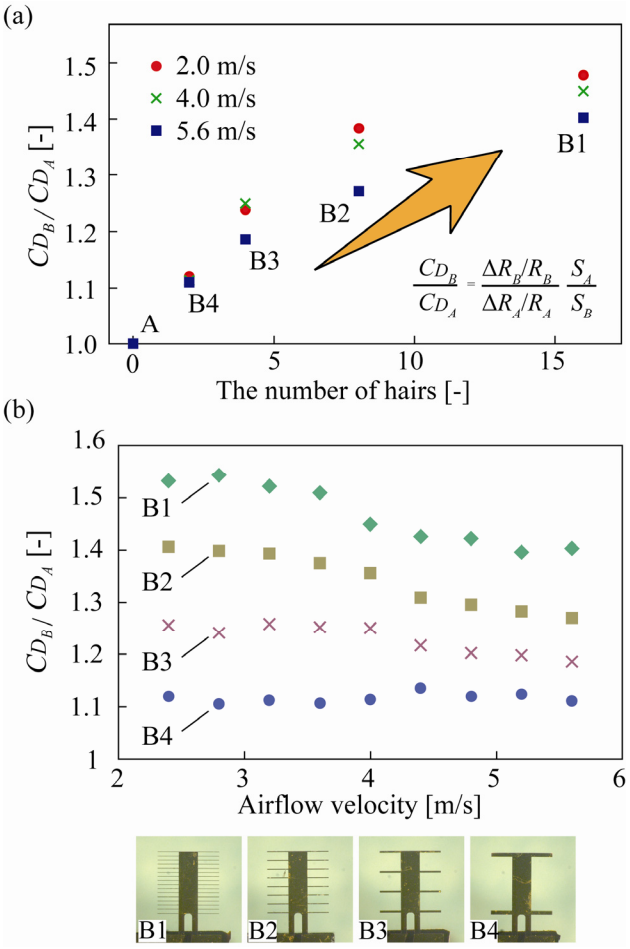

Figure 7: (a) Relationship between number of hairs and ratio between drag coefficient of Cantilever A and B (=C_{D_B}/C_{D_A}). (b) Relationship between airflow velocity and C_{D_B}/C_{D_A}.

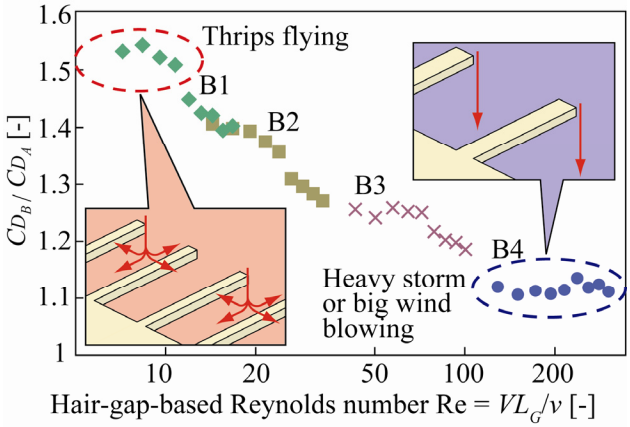

Figure 8: Relationship between hair-gap-based Reynolds number and C_{D_B}/C_{D_A}.

CONCLUSION

In conclusion, we confirmed that the bristled wing acted as an imaginary airflow block at low Reynolds number. Around low Reynolds number of thrips flying, C_{D_B} was 1.5 times larger than C_{D_A}. In contrast, C_{D_B} was approximately same as C_{D_A} at Re>100. These results indicate that a thrips utilizes this aerodynamic phenomenon to obtain aerodynamic force efficiently.

ACKNOWLEDGEMENT

The photolithography masks were made using the University of Tokyo VLSI Design and Education Center (VDEC)'s 8 inch EB writer F5112 + VD01 donated by ADVANTEST Corporation.

REFERENCES

[1] A. P. Willmott, *et al.*, "Measuring the angle of attack of beating insect wings: robust three-dimensional reconstruction from two-dimensional images," *Journal of Experimental Biology*, vol. 200, pp. 2693-2704, 1997.

[2] E. I. Fontaine, *et al.*, "Wing and body motion during flight initiation in Drosophila revealed by automated visual tracking," *Journal of Experimental Biology*, vol. 212, pp. 1307-1323, 2009.

[3] E. I. Dickinson, *et al.*, "Wing rotation and the aerodynamic basis of insect flight," *Science*, vol. 284, pp. 1954-1960, 1999.

[4] C. P. Ellington, *et al.*, "Leading-edge vortices in insect flight," *Nature*, vol. 384, pp. 626-630, 1996.

[5] C. P. Ellington, *et al.*, "Wing mechanics and take-off preparation of Thrips (Thysanoptera)," *Journal of Experimental Biology*, vol. 85, pp. 129-136, 1980.

[6] S. Tanaka, *et al.*, "Thrips' flight. Part 1," *in Symposia '95 of Exploratory Research for Advanced Technology*, Japan Science and Technology Corporation, pp. 27-34. 1995.

[7] S. Sunada, *et al.*, "Fluid-Dynamic characteristics of a bristled wing," *Journal of Experimental Biology*, vol. 205, pp. 2737-2744, 2002.

[8] H. Takahashi, *et al.*," Differential pressure sensor using a piezoresistive cantilever," *Journal of Micromechanics and Microengineering*, vol. 22, pp. 055015, 2012.

[9] N. Minh-Dung, *et al.*, "3D airflow velocity vector sensor," *Proceedings of 24th International Conference on Micro Electro Mechanical Systems*, pp. 513-516, 2011.

CONTACT

*Ken Sato, tel: +81-3-5841-0461;
satou@leopard.t.u-tokyo.ac.jp